scientific reports



OPEN

Impact of carbon nanotubes on chloride diffusion in cement mortar under temperature gradient conditions

Sohail Magsood¹, Mohd Mukarram Ali^{1,3}, Remilekun A. Shittu² & Tae-Yeon Kim^{1,2,3} ⊠

Reinforcement corrosion induced by chloride ingress is a major durability issue in cementitious materials, particularly in harsh marine environments. Incorporating carbon nanotubes (CNTs) has emerged as a promising solution to mitigate chloride ingress. However, their performance against chloride diffusion under elevated temperatures remains unexplored. This study explores the influence of adding CNTs in cement mortars, aiming to mitigate chloride ion diffusion under temperature gradient conditions. CNTs were incorporated at 0.05%, 0.10%, and 0.15% by weight of cement in mortar specimens. Specimens were exposed to a 3% NaCl solution at room temperature of 22 °C (CT22), a high ambient temperature of 50 °C (CT50), and under a temperature gradient (TG). The experiment was carried out in two stages: the first stage aimed at finding the optimal mix based on the compressive strength, absorption, porosity, and total chloride concentration profile under the TG condition, whereas the optimal mix was thoroughly analyzed under different temperature conditions along with the assessment of the free chloride concentration profile in the second stage. The results indicated that adding 0.05% CNTs yielded the best performance, showing over a 24.6% increase in strength, about 17.5% reduction in absorption and accessible porosity, improved porous structure, and reduced chloride content. Notably, the critical chloride content based on the accelerated laboratory experimental results was substantially lower in the optimal mix than in the control, suggesting that 0.05% CNTs effectively delays chloride ion diffusion and corrosion initiation, enhancing the durability in marine environments.

Keywords Cementitious composites, Carbon nanotubes, Compressive strength, Transport properties, Temperature, Total chlorides, Free chlorides, Critical chloride content, Porosity

Reinforcement corrosion in concrete is one of the commonly observed deterioration types in hot and aggressive marine environments, such as the Middle East and North Africa (MENA) regions. It typically occurs due to either chloride ingress or carbonation in concrete, while chloride ions are more detrimental as compared to carbonation¹. Moreover, the chloride ions usually interact with the rebar in cementitious materials through diffusion, moving along a concentration gradient inside a continuous liquid phase². This penetration rate usually depends on the quality of cement composites, chloride binding ability, exposure duration, hydration level, temperature, and presence of additives²⁻⁶. Previous studies^{7,8} revealed that high ambient temperature is one of the most significant causes of accelerating chloride ion diffusion. The increase in temperature causes the release of bound chlorides into the pore solution, which increases the accumulation of free chlorides in the cementitious materials, leading to corrosion initiation. The most prevalent temperature condition in an aggressive marine environment is the temperature gradient (TG) across the concrete section⁹⁻¹¹. It creates a driving force for diffusion species like chlorides, a phenomenon termed as Soret effect¹². The differential temperature causes kinetic energy to fluctuate between the hotter and colder regions of the concrete, leading chloride ions to migrate from the hotter region and accumulate in the cooler part. Such a type of diffusion has a double driving force due to both mass diffusion and thermo-diffusion¹³. To reduce the chloride diffusion, transport properties such as porosity and absorption of the cement mortar should be minimized by incorporating appropriate additives.

¹Department of Civil and Environmental Engineering, Khalifa University of Science and Technology, Abu Dhabi 127788, UAE. ²Emirates Nuclear Technology Center, Khalifa University of Science and Technology, Abu Dhabi 127788, UAE. ³Advanced Digital & Additive Manufacturing Group, Khalifa University of Science and Technology, Abu Dhabi 127788, UAE. [∞]email: taeyeon.kim@ku.ac.ae

Nanomaterials have garnered significant focus for improving durability by enhancing transport properties^{14,15}. Moreover, they contribute to the cement matrix by filling gaps, strengthening bonding between particles, and providing crack-bridging action, thus improving the performance of cement composites^{16–19}.

Researchers have explored the addition of nanomaterials to improve the resistance to chloride ion diffusion of cementitious composites. For instance, Meddah et al.²⁰ reported a 29% rduction in chloride penetration by adding 3% nano-alumina particles. This resistance was correlated to the formation of supplemental calcium-silicate aluminate hydrate, pore refinement, and microstructural densification due to nano-alumina in the cement matrix. Zhang and Li²¹ concluded that the incorporation of nano-silica and nano-titanium up to 1% reduced chloride ion penetration by 30%, though higher dosages led to agglomeration and voids in the cement matrix. Wang et al.²² found that incorporating modest amounts of modified graphene nanosheets (0.02 wt%) into cement paste reduced chloride ion penetration depth by 37%, when compared to the reference mix. This improvement was attributed to the filling and crack-preventing capabilities of graphene nanosheets in the cement matrix.

Among the carbon-based nanomaterials, carbon nanotubes (CNTs) are an inexpensive solution to enhance the properties of concrete due to their multifunctionality²³, usage in lower quantities²⁴, and the decreasing cost of base nanomaterials²⁵. They are rolled graphene sheets consisting of graphite as a basic unit. Besides, multiwalled carbon nanotubes (MWCNTs) are less expensive than single-walled carbon nanotubes (SWCNTs) and are suitable for enhancing the mechanical properties of cementitious materials because of their greater stiffness²⁶. Previous studies revealed that CNTs are effective against the ingress of chloride ions along with the improvement in the strength of the material, while different studies indicate different effective dosages of MWCNTs for better performance. For mortar, a 0.4% dosage improvs the chloride diffusion coefficient²⁷; however, another study reports up to a 50% reduction in chloide content at a 0.1% dosage²⁸. Similarly, a concrete mix with a 1% dosage has been recomended for the lowest chloride penetrability based on the charge passed as per ASTM equivalent (coulombs)²⁹. Regarding special-purpose concrete, ultra-high-strength concrete with a 0.05% dosage can cause a 24% rduction in the chloride diffusion coefficient³⁰, and ultra-high-performance concrete with 0.25% and 0.05% CNTs reduces the cloride difusion coefficient³¹. Moreover, 0.25% pristine, 0.5% hydroxyl-functionlized, and 0.25% helical MWCNTs have also been recommended for the improved chloride resistance of ultra-highperformance concrete³². CNTs-based composites are chloride resistant because of refined porosity and the crack-bridging quality in the cementitious matrix¹⁶⁻¹⁹ provided that the CNTs must be properly dispersed in the cement paste^{18,33}. The refined porosity in CNTs-based cementitious material is primarily due to the nucleation and filler effects¹⁹. Consequently, the formation of more nucleation sites results in a denser microstructure of C-S-H, necessary for reduced porosity and improved durability^{34,35}. Additionally, such cementitious materials with a denser microstructure and reduced porosity also cause improved transport properties and enhanced resistance against chloride ingress³⁶.

The dispersion of CNTs in water can be done through physical (sonication, mechanical mixing, and magnetic stirring), and chemical (dispersant or surfactants), but it is recommendable to employ the combination of both methods³⁷. The use of polycarboxylate superplasticizers as a dispersant is a good choice because of their ability to maintain workability along with facilitating dispersion of CNTs³⁸. Pristine CNTs are hydrophobic in nature and prevent the proper dispersion of CNTs in aqueous suspension, but it can be overcome through some covalent and non-covalent treatments³⁹. Non-covalent surface treatments with polyethylene glycol (PEG), for example, make the CNTs more hydrophilic by encouraging surface adsorption, which improves their dispersion and stability in aqueous solutions^{39,40}. A study also reported that the presence of PEG as a chemical admixture reduces the chloride binding capacity of the cementitious matrix by compromising the microstructure and morphology of calcium silicate hydrate (C-S-H)⁴¹. However, the compressive strength enhances when PEG is used as a surface treatment on CNTs, even at a low dosage⁴². Moreover, PEG-treated CNTs also contribute to a reduction in chloride permeability, likely due to better dispersion and improved interaction with the cementitious matrix⁴³.

Although CNTs enhance chloride resistance in cement composites, their effectiveness under high ambient temperature and TG conditions remains largely unexplored. This study examines the use of CNTs to reduce chloride ion diffusion in cement composites, focusing on harsh marine environments that involve elevated temperatures. This reflects the performance of CNTs-based cementitious composites in a chloride-rich environment, where temperature is an influential factor in accelerating chloride-induced corrosion, such as in the coastal areas of the MENA region. The MENA region experiences extremely high temperatures during peak summers. For example, the UAE's average maximum temperature of 20 years reaches 43.3 °C during August⁴⁴.

The present work investigates the chloride resistance potential of cementitious mortar by incorporating MWCNTs treated with PEG under different temperature conditions. The choice of using PEG-treated CNTs was due to their superior dispersion, long-term stability, and enhanced mechanical properties 39,40,42,45. The methodology comprised determining the optimal concentration of PEG-treated MWCNTs in the mix by considering the mechanical and transport properties in the first stage, such as compressive strength, absorption, porosity, and chloride diffusion profile under TG. In the second stage, the mix with the optimal concentration of MWCNTs was thoroughly investigated against chloride diffusion under high ambient temperature and TG conditions, as well as for free chlorides under TG conditions to assess the corrosion initiation potential. For chloride exposure, each cylindrical specimen, with a diameter of 96 mm and a height of 80 mm was enclosed in an acrylic tube and sealed to ensure only unidirectional flow from the bottom side. Each specimen was fully immersed in a 3% NaCl solution under isothermal conditions, whereas only the bottom surface was exposed to the solution under TG conditions. Additionally, results were presented in the form of chloride concentration profiles and were related to strength, porosity, and absorption to justify the enhanced chloride diffusion resistance of the optimal mix.

Description	Requirements as per BS EN 197-1:2011	Typical results		
Fineness: Blaine air permeability (m²/kg)		310-330		
Specific gravity		3.13-3.14		
Soundness: Le Chatelier exp., mm	≤ 10	0.10-0.15		
% Standard consistency		26.0-28.0		
Time of setting: Vicat test				
Initial, minutes	≥ 60	180-190		
Final, minutes		220-230		
Compressive strength, MPa				
2 Days	≥ 10	22-26		
7 Days		38-42		
28 Days	≥ 42.5 ≤ 62.5	48-52		

Table 1. Physical properties of cement.

Description	Requirements as per BS EN 197-1:2011	Typical results
% Loss on ignition	≤ 5.0	3.40-3.50
% Insoluble residue	≤ 5.0	0.20-0.40
% SiO ₂		19-21
% Al ₂ O ₃		5.0-5.2
% Fe ₂ O ₃		3.2-3.4
% CaO		63-64
% MgO		1.3-1.5
% SO ₃	≤ 3.5	2.4-2.6
% Na ₂ O equivalent		0.4-0.7
% Cl	≤ 0.10	0.01-0.03
% Free CaO		1.0-2.0
% C ₃ S		53-55
% C ₂ S		15-17
% C ₃ A		7-9
% C ₄ AF		9-11

Table 2. Chemical composition and Bogue's components of cement.

Methodology Materials

The binder used in this study was Ordinary Portland Cement (OPC), designated as CEM I 42.5 N as per specifications of BS EN 197-1. The detailed physical properties and chemical compositions of this cement are tabulated in Tables 1 and 2, respectively. Aggregates used were the blend of fine dune sand (DS) and fine crushed sand (CS), with a maximum size of 0.6 mm. The fineness modulus of both sands was found to be 1, as per the ASTM C136 procedure⁴⁶. Using a blend of DS and CS is a cost-effective and environmentally friendly approach that results in better fresh properties, strength, and durability^{47–49}. Furthermore, the detailed gradation curve for both sands is shown in Fig. 1. Although both sands consist of fine particles, DS has a relatively smoother curve with a lower proportion of coarser particles. However, both sands are comparable and show slight variation. Deionized water was used because the primary concern of this study is chloride ion diffusion.

The CNTs used in this study were multi-walled in the form of flakes which are less hazardous for human health, available with the product code ANS-ECF-01-000-PEG01, and procured from Applied Nanostructured Solutions, LLC (USA), a spin-off company of Lockheed Martin Corporation. The CNTs consist of glass fiber as a substrate medium during the growth of CNTs, and PEG as a dispersing agent as mentioned in Table 3. To make the suspension of CNTs in water, polycarboxylate ether (PCE) superplasticizer (SP) was used as a dispersant which satisfies the requirements of Type A, Type E, and Type F admixtures as per ASTM C494⁵⁰ which improves the workability and the dispersion³⁸. The detailed specifications of PCE are listed in Table 4.

In addition to the above-mentioned materials, analytical reagents were also used to determine the total and free chloride contents in mortar samples by using precipitation titration^{51,52}. The detailed purpose and specifications of these reagents are described in Table 5.

Mix designs and experimental procedure

The mix proportions in this study were designed based on the standard mortar as per ASTM C109⁵³ along with some modifications on account of using a blend of DS and CS. These modifications involved adjusting the water-to-cement ratio (w/c) and the SP content to ensure consistent flow across all mixtures. Ultimately, the w/c

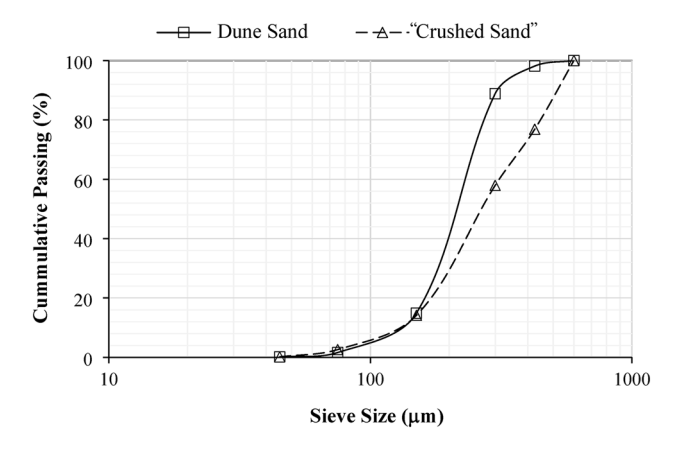


Fig. 1. Gradation curve for dune and crushed sands.

Component	Specification
MWCNTs	>93%
Fiberglass	<1%
Polyethylene glycol (PEG)	<6%
Length of MWCNTs range	1–500 μm
The diameter of MWCNTs range	9–16 nm
Purity	>99.8%

Table 3. Specifications of CNTs.

Description	Specification
Appearance and form	Whitish to light brownish liquid
Specific gravity at 25 °C	1.060 typical
pH-value at 25 °C	4-7
Chloride ion content ≤	≤ 0.01%
Alkali content (Na ₂ O equivalent %)	<3%

Table 4. Specifications of PCE.

Reagent	Purpose	Specifications
Nitric acid (HNO ₃)	Solvent for sample dissolution	65% purity
Silver nitrate (AgNO ₃)	Chloride titration	≥ 99.9% purity
Sodium chloride	Standard solution preparation	≥ 99.5% purity
Methyl orange	Titration indicator	Suitable for analytical use
Water	Solvent and diluent	Reverse osmosis water (Type III - ASTM D1193)

Table 5. Details of analytical reagents.

ratio was set at 0.60, and the SP dosage was fixed at 0.5% fr CNT-based mixes only. The dosages of CNTs were varied at 0.05%, 0.10%, nd 0.15% b weight of cement, as shown in Table 6. This mix proportion resulted in a consistent flow of $35\% \pm 5\%$ for all the mixes, in accordance with the procedure described in ASTM C1437⁵⁴. To prepare a well-dispersed suspension of CNTs in deionized water, sonication was done at 20 kHz for a total duration of 30 min in three parts duration and at a constant amplitude of 40%. Each part lasted for 10 min along with a break of 5 min between two consecutive parts. The entire sonication process was aided with the constant magnetic stirring⁵⁵. Sonication was done using Sonics Vibra-Cell VC750 ultrasonic liquid processor along with delivering > 18,000 joules energy under 30–33 watts. Sun et al. ⁵⁶ also considered the energy delivered and power to get the well-dispersed suspension for marine concrete. Moreover, Fig. 2 below depicts the complete sonication process, including CNTs suspension before and after sonication.

Mix	OPC (kg/m ³)	CS (kg/m ³)	DS (kg/m ³)	Water (kg/m³)	CNTs (kg/m ³)	SP (kg/m ³)
M-C	506	695.5	695.5	303.5	-	-
M-0.05CNT	506	695.5	695.5	303.5	0.253	2.53
M-0.10CNT	506	695.5	695.5	303.5	0.506	2.53
M-0.15CNT	506	695.5	695.5	303.5	0.759	2.53

Table 6. Details of mix proportions expressed in weight.

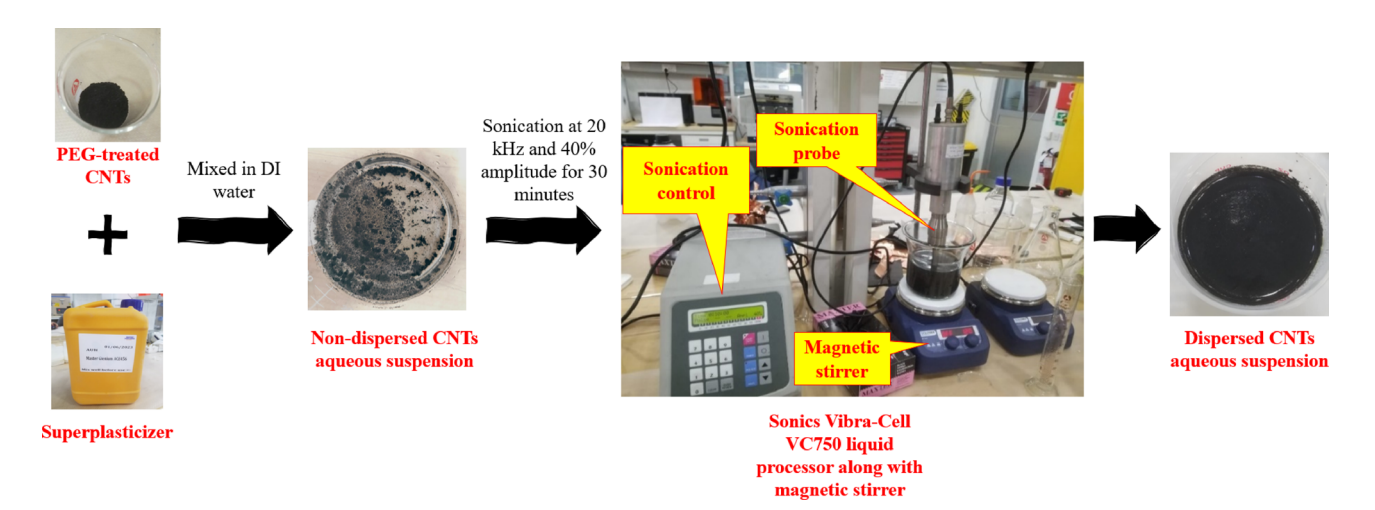


Fig. 2. Flow diagram showing the steps of the sonication process.

Furthermore, the experimental methodology was conducted in two stages. The first stage aimed to determine the optimal mix proportion by adding CNTs, while the second stage involved a detailed investigation of the chloride content in the obtained optimal mix. Notably, the optimal mix proportion was determined based on compressive strength, cumulative absorption within 72 h, porosity from the backscattered electron (BSE) image analysis, and total chloride content under temperature gradient conditions. For the detailed analysis of chloride content in the second stage, the total chloride concentration was found at constant room temperature and constant high ambient temperature conditions. Additionally, free chloride content was also found for the temperature gradient condition. The specimens were Ø96 mm x 80 mm cylindrical in shape, cast in custommade acrylic molds as shown in Fig. 3. This specimen size has also been reported in the literature for chloride diffusion analysis^{57–59}. Additionally, 50 mm cubic specimens were prepared exclusively for compressive strength. Three cubic specimens were tested for each mix to determine the compressive strength, while two cylindrical specimens were tested for the absorption test and for each temperature condition for chloride diffusion analysis. Averages of these results were presented and discussed in Sect. 3.

For chloride diffusion analysis, cylindrical specimens were exposed to a 3% NaCl solution for 30 days under three different conditions: constant room temperature of 22 °C (CT22), constant high temperature of 50 °C (CT50), and temperature gradient (TG) conditions, as schematically shown in Fig. 4. The top surface and the bottom circumferential gap of the specimens were sealed using silicone sealant after placing them into the acrylic tubes to ensure a one-dimensional flow of the 3% NaCl solution from the bottom surface. These enclosed specimens were then placed in a temperature-controlled 3% NaCl solution bath to impose either constant or varying temperature conditions. The specimens were fully submerged in the 3% NaCl solution to ensure constant temperature conditions (see Fig. 4a, b). To create a temperature gradient across the depth of the specimens, only the bottom surface was exposed to the 3% NaCl solution at 50 °C, while the top surface was exposed to room temperature of 22 °C, as shown in Fig. 4c. All the 3% NaCl solution baths were covered with aluminum foil to minimize water loss due to evaporation. To record the temperature gradient, three K-Type thermocouples were installed at distances of 10 mm, 30 mm, and 40 mm from the chloride exposed (bottom) surface as shown in Fig. 4c.

Stage I—determination of optimal mix

The optimal mix was determined based on the results of the compressive strength, absorption test, porosity analysis, and total chloride content analysis under the TG condition. Compressive strength is one of the primary methods for assessing the quality of cementitious materials, as it reflects structural capacity and durability³¹. The compressive strength of cubic specimens was measured on the 7th and 28th days of curing using an MTS machine with a load capacity of 300 kN. The test was conducted according to ASTM C109⁵³. The compressive strength was determined using

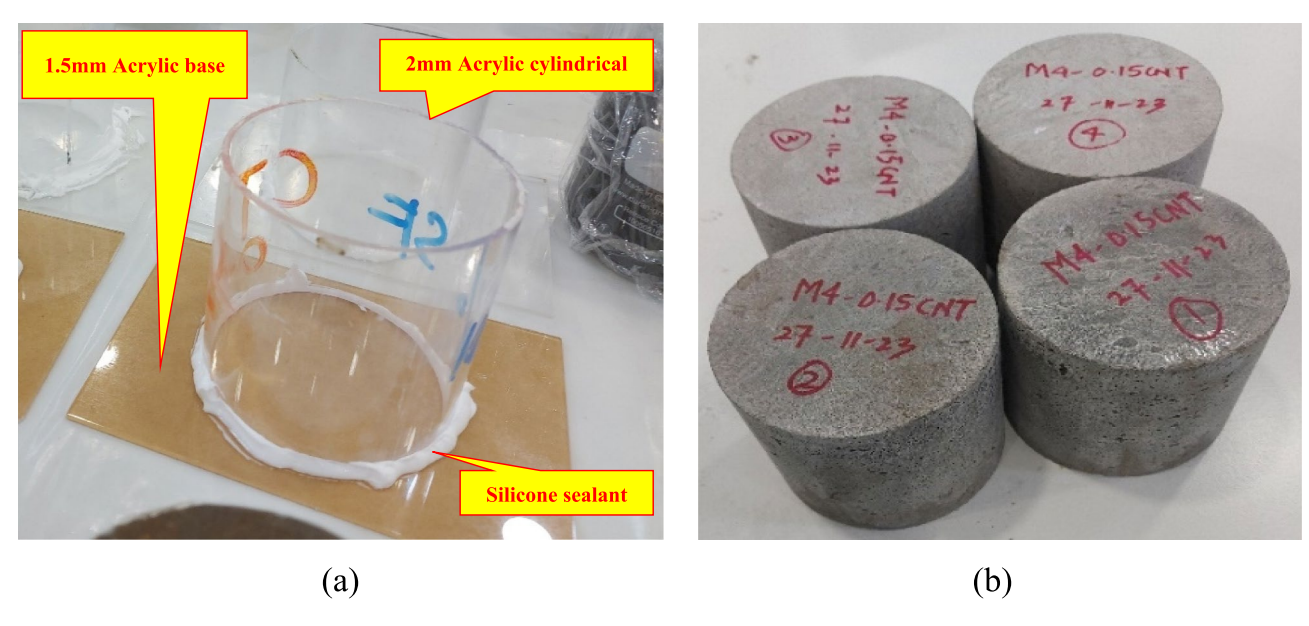


Fig. 3. Preparation of cylindrical specimens: (a) custom-made acrylic mold sealed with silicon sealant at the bottom to check the leakage of water and cement and (b) cylindrical specimens with 96 mm diameter and 80 mm depth.

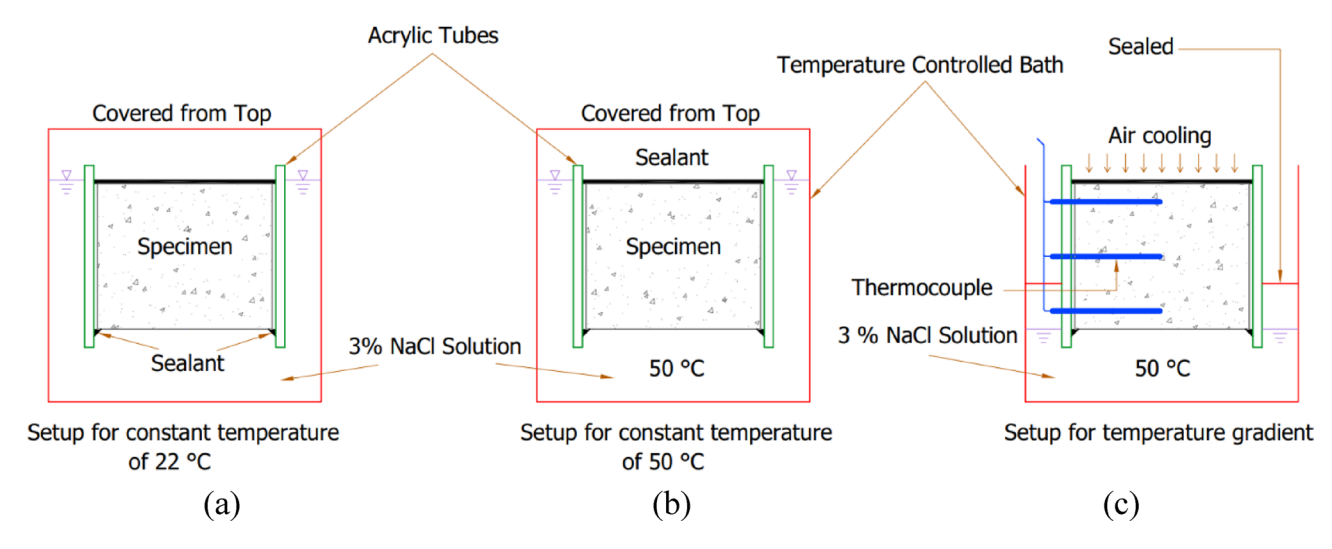


Fig. 4. Experimental setup for three temperature conditions: (a) CT22, (b) CT50, and (c) TG.

$$Compressive strength = \frac{F}{B \times D}.$$
 (1)

where F, B, and D are maximum compressive force, width and depth of the specimens.

Water absorption in cementitious composites is a significant indicator of overall durability, since the faster water penetrates the material, the more prone it is to harmful ions and other durability issues⁶⁰. The absorption test was performed on the dried cylindrical specimens, which were used in chloride diffusion analysis. A procedure consisted of fully immersing the specimen in deionized water to determine permeable porosity, as reported in the literature^{61–63}. For this purpose, each specimen was dried at 105 °C in an oven until the weight loss became negligible. While drying cement mortar specimens at 105 °C may cause minor alterations in the microstructure, it is a widely accepted practice recommended by several standards, including ASTM. Although ettringite begins to decompose at around 60 °C⁶⁴, its presence in 28-day-old hardened cement paste is minimal^{65,66}. The primary hydration product, calcium silicate hydrates (C-S-H), remains stable until temperatures exceed 180 °C⁶⁷, indicating that the overall microstructure of the mortar remains largely intact at 105 °C. Furthermore, the potential influence on water absorption measurements is negligible due to the higher aggregate content and lower cement paste volume in the mortar mix.

After that, the specimen was fully immersed in the deionized water until the weight gain became constant. It took 48 h to dry and 72 h to get full absorption in the cylindrical specimens. The results were presented in the form of absorption and permeable/accessible porosity. The permeable/accessible porosity in percentage 68 was computed by

$$\phi_P = \frac{\triangle W \times v_w}{1000 \times V} \times 100, \tag{2}$$

where ϕ_P is the permeable or accessible porosity (%), $\triangle W$ is cumulative absorption of water after 72 h (g), v_w is the specific volume of water taken as 10^{-3} m³/kg, and V is the volume of the specimen (m³). To assess the porosity, BSE images for each gold-coated specimen (< 5 mm in size) were taken at 2500 times magnification and 5 kV accelerated voltage using a Phenom XL Desktop Scanning Electron Microscope (SEM). This kind of electron microscope facilitates easy and rapid switching between secondary electron mode and backscattered electron mode, enabling fast and efficient analysis. Unlike typical BSE, the specimens used were unpolished and non-epoxy impregnated. This was done because images were captured both in secondary electron mode and BSE mode, but BSE images were selected for binary image analysis due to their superior contrast and clear depiction of surface roughness. The primary focus of this procedure was to perform a qualitative analysis of pore sizes, shapes, and distribution. These images were later analyzed in Fiji Software developed by the USA-based National Institute of Health (NIH). In this software, an 8-bit BSE image was converted into a 2-channel (binary) image to highlight the solids and the pores for the detailed analysis of porosity.

To determine the total chloride content, a 36 mm core was extracted from the exposed specimens and sliced into 10 mm layers, excluding the top and bottom 5 mm layers, as shown in Fig. 5. Each layer was then pulverized and passed through an 850-micron sieve. These pulverized samples were used to measure the acid-soluble (total) chloride content using the standard approach defined in ASTM C1152, which is based on precipitation titration⁵¹. Finally, the optimal mix was chosen based on the compressive strength, absorption, porosity, and total chloride content under TG conditions. This optimal mix was further analyzed under all temperature conditions and compared with the control mix.

Stage II—detailed chloride diffusion analysis of optimal mix

In this stage, a similar sample extraction procedure was adopted for the specimens of the optimal mix exposed to constant temperature, as shown in Fig. 5. Likewise, the total chloride content was determined in each layer as per ASTM C1152 and compared with the control specimen. Moreover, the specimens under the TG condition were also analyzed for free chlorides using the standard procedure as per ASTM C1218⁵². The purpose of finding the free chlorides was to determine the potential of releasing chloride ions in the pore solution.

Results and discussions Stage I—determination of optimal mix

Compressive strength

The effect of incorporating CNTs on compressive strength was examined to determine the optimal mix. The results in Fig. 6a show a 0.05% CNTs as an optimal dosage, resulting in the highest compressive strength after 7 days and 28 days of curing. Figure 6b shows the relative compressive strength of all specimens compared to the control mix, calculated using Eq. (3). An increase in the compressive strength for a 0.05% CNTs dosage is 24.63% after both 7 days and 28 days. This improvement is due to the reinforcing action of CNTs, which bridge nanoscale cracks and regulate their propagation in the cement matrix¹⁶. Moreover, the higher dosages (i.e., 0.10% ad 0.15%) how a decrease in the compressive strength results. For instance, after 28 days, the compressive strength of 0.10% and 0.15% reduces by 22.57% and 29.86%, respectively, when compared with the control mix.

$$Relative\ Compressive\ strength = \frac{Compressive\ strength\ of\ a\ mix\ containing\ CNTs}{Compressiev\ strength\ of\ a\ control\ mix}. \tag{3}$$

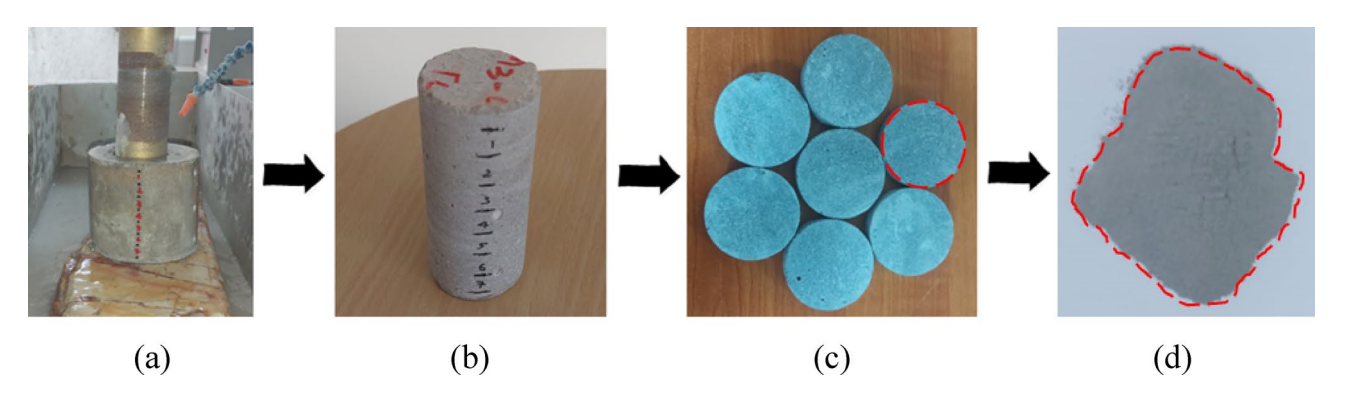
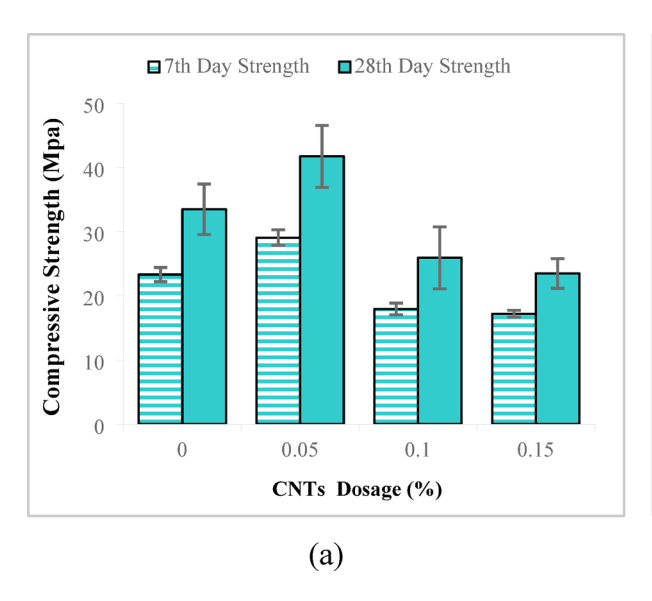


Fig. 5. Sample preparation for chloride diffusion analysis; (a) Core extraction, (b) 36 mm core, (c) Sliced core, and (d) pulverized and sieved sample.



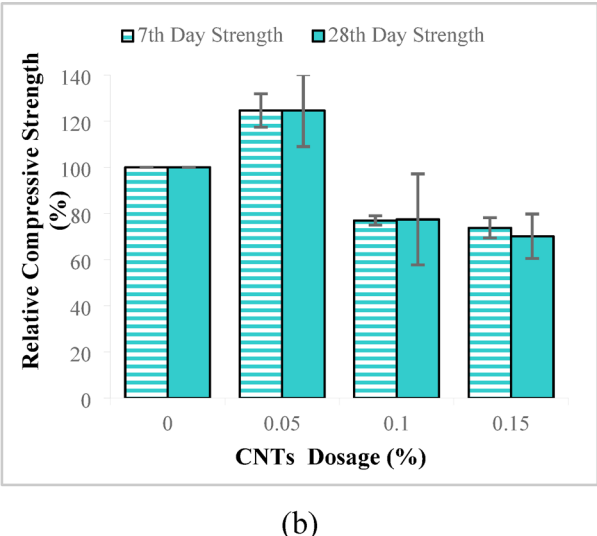
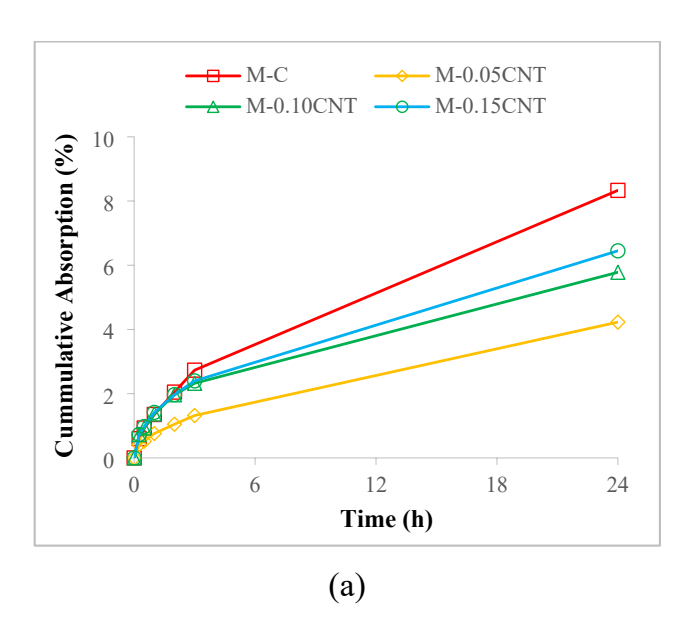


Fig. 6. Variation in the compressive strength at different dosages of CNTs: (a) Compressive strength and (b) Relative compressive strength.



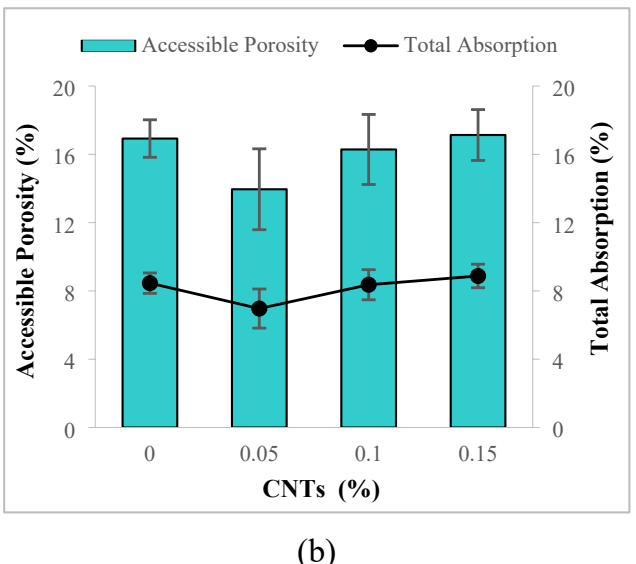


Fig. 7. Absorption test results: (a) cumulative water absorption within the first 24 h and (b) total absorption vs. accessible porosity after 72 h of absorption period.

The previous study⁶⁵ reported that CNTs dosages below 0.5% resulted in a 5–40% increase in the 28-day compressive strength, with lower water-to-binder (w/b) ratios requiring a lower CNTs dosage to achieve maximum strength improvement. In the current study, the compressive strength increase at the optimal dosage is more than 24%, which falls within the reported range. However, this case differs in terms of water content due to the use of DS and CS as fine aggregates, which requires a higher w/c ratio than other sands because of its fine particle size and larger surface area^{48,49}. Despite a high w/c ratio (i.e., w/c=0.6), the flow values remain low, around 35% \pm 5%, indicating that the optimal dosage identified may correspond to mixes with a lower w/c ratio using other types of sand as reported in the literature. Therefore, the results presented in Fig. 6 align with those for mixes with low w/b ratios of 0.4 and 0.2 reported in previous studies^{30,69,70}. The reduction in strength at higher CNTs concentrations could be attributed to the agglomeration of CNTs in the cement matrix⁷⁰.

Absorption and accessible porosity

The cumulative absorption after 24 h for each mix is shown in Fig. 7a, whereas the total absorption of water after the full absorption period (i.e., 72 h) and the accessible porosity are shown in Fig. 7b. The addition of CNTs resulted in lower water absorption within the first 24 h, as shown in Fig. 7a, demonstrating the improved

durability of CNTs-based cement mortar against chloride diffusion. Among the CNTs dosages, 0.05% CNTs has been proven as an optimal dosage because of the lowest water absorption value. In Fig. 7b, 0.05% CNTs show the lowest water absorption and least accessible porosity of 6.97% and 13.95% after 72 h, respectively. These values represent a reduction of more than 17.50% compared to the control mix. Furthermore, the higher CNTs dosages show comparable results with the control mix. Therefore, 0.05% CNTs can be considered as an optimal dosage based on the transport properties, including total absorption and accessible porosity.

CNTs in cementitious materials have been reported to refine porosity and reduce water absorption ^{19,71,72}. Nochaiya and Chaipanich⁷³ found that while incorporating CNTs does not significantly reduce the total porosity of a cementitious matrix, it decreases the overall connectivity of the matrix through a bridging effect, leaving macro pores largely unaffected. Despite this, CNTs refine porosity through mechanisms such as nucleation and the filler effect¹⁹. As a result, the total volume of permeable pores does not change significantly, leading to a gradual decrease in the relative change in water absorption over time, as shown in Fig. 8. This indicates that, if absorption continues beyond 72 h, the relative change could become insignificant and comparable to the control mix. The positive relative change indicates a decrease in absorption, whereas the negative relative change reflects an increase in absorption. The mix with 0.05% CNTs indicates relatively the highest decrease in absorption over the period of 24, 48, and 72 h, while the higher dosage, such as 0.15% CNTs, causes the lowest decrease and even an increase in absorption compared to the control mix after 72 h. The CNTs network within cementitious materials creates intricate and convoluted paths for water movement, reflecting higher tortuosity, which enhances the durability of the material⁷⁴. Additionally, the total volumetric absorption rate shown in Fig. 9 further indicates increased tortuosity. The control mix displays a regular absorption curve, while the irregular curves of the CNTs-based mixes suggest that water follows a more convoluted path due to increased tortuosity.

Pore structure and distribution

The findings of the compressive strength and absorption tests can be validated by visually examining the pores through microstructural analysis. Figure 10 displays a comparison of BSE images and their binary images for each specimen, each with a different amount of CNTs. This comparison demonstrates how the pore structure of the material is affected by the inclusion of CNTs. At 2500 times magnification, the images mostly display active pores (smaller than 10 μm) that are involved in transport mechanisms. Additionally, only images without any signs of air voids were selected. It can be observed that the porosity reduces by adding 0.05% CNTs according to both BSE and binary images, whereas the porosity of the other dosages is comparable to that of the control mix. This observation supports the claim made in the preceding section that a dosage of 0.05% CNTs results in enhanced compressive strength and reduced water absorption due to lower porosity. Moreover, it can be observed that the pores in the control mix are regular in shape and well-distributed compared to the CNTs-based mixes. However, the 0.05% CNTs-based mix performed optimally due to its smaller-sized and less dense pores.

The presence of smaller pores, with a radius of less than 10 nm, does not have a substantial impact on strength, as they contribute negligibly 75 . However, the total volume of pores, and specifically the larger pores can negatively impact the compressive strength 76 . Taking this into account, the reduction in the compressive strength at higher CNTs dosages (i.e., 0.10% and 0.15%) are primarily due to the presence of large-sized pores in these mixes. Additionally, the non-uniform pore distribution can also reduce the strength due to the presence

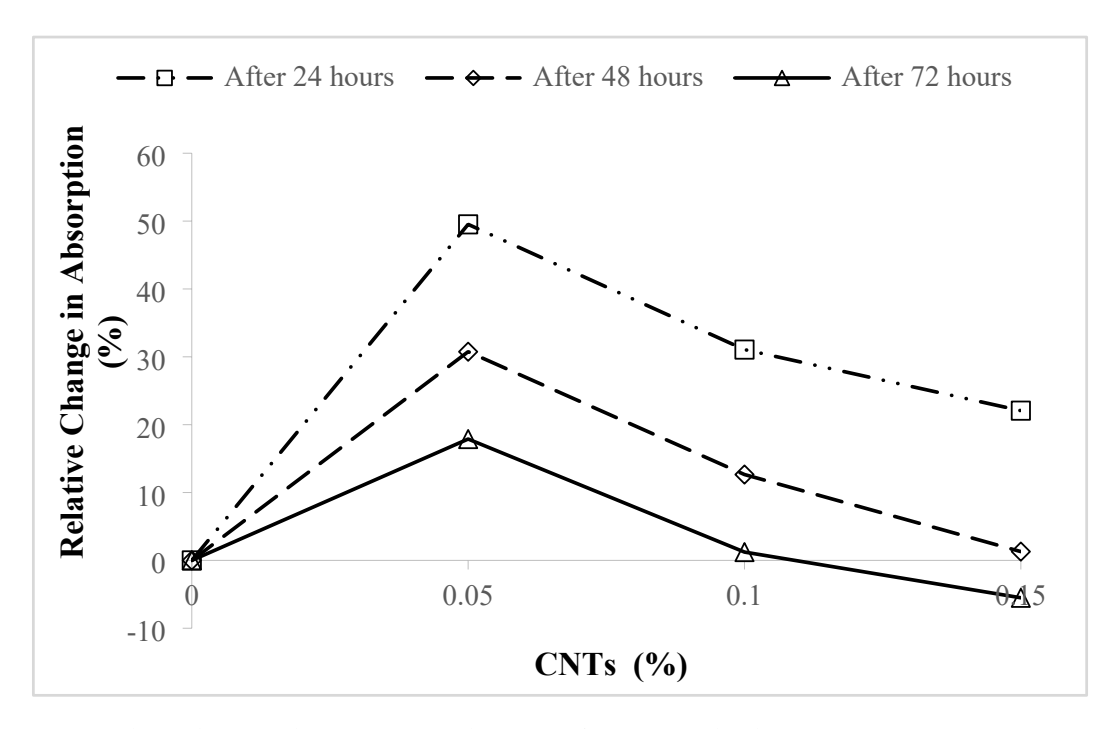


Fig. 8. Relative change (reduction) in water absorption after 24, 48, and 72 h.

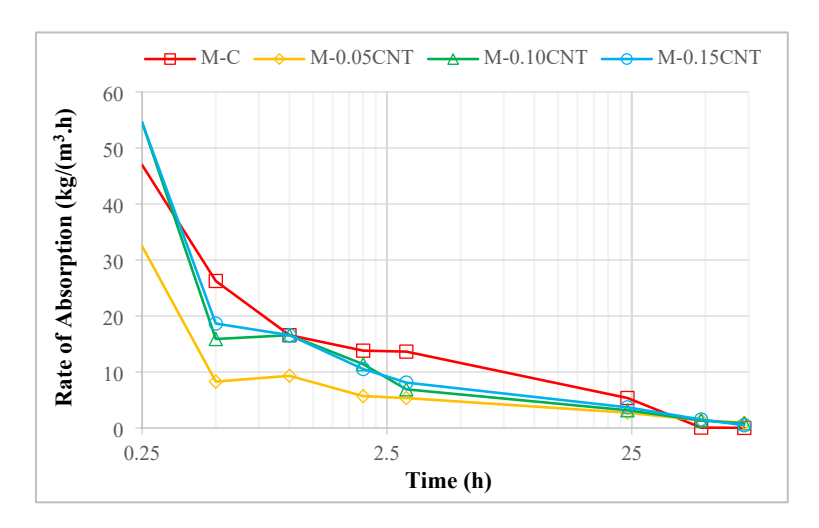


Fig. 9. Variation in volumetric water absorption rate over a period of 72 h.

of weaker zones⁷⁷. Therefore, this reason is another justification for the reduction in the compressive strength at higher CNTs dosages because they showed a non-uniform distribution of pores as compared to the control mix (Fig. 10). For the optimal mix (i.e., 0.05% CNTs), while the pore distribution is not uniform, the pores are smaller in size compared to the control mix, leading to an improvement in compressive strength.

The transport properties of cementitious materials are significantly influenced by their microstructure, particularly the porosity and connectivity of pores within the material 11 . The porosity characteristics (i.e., size, shape, and distribution of pores) have an impact on the transport mechanism of the cementitious materials. For example, smaller pores (i.e., active pores < $10~\mu m$) act as channels that facilitate the transport process 78 . However, the amount of water absorbed is determined by the total volume of pores in the mixture. Higher water absorption results from larger pores because they retain water in the form of pore solution rather than participating in the transport mechanism 79 . Therefore, at higher CNTs dosages, larger pores cause increased water absorption. Furthermore, tortuosity is increased by the non-uniform distribution of pores and their variable pore shape in the cementitious matrix 80 . The porosity is reduced with the addition of 0.05% CNTs, which leads to stronger and less absorbent cementitious materials. However, the transport mechanism through CNTs-based mixtures is hampered by the irregular pore shapes, non-uniform distribution of pores, and reduced connectivity. This leads to higher tortuosity, which indicates improved durability. At higher CNTs dosage, however, the presence of larger pores reduces both durability and strength.

Total chloride content under the TG condition

The thermocouple readings were recorded after the specimens were exposed to 3% NaCl solution for 30 days. The average readings at designated depths of 10 mm, 40 mm, and 70 mm from the chloride exposed surface are represented in the form of a temperature gradient in Fig. 11. It can be observed that the temperature profile along the depth is nearly identical for all specimens. Furthermore, the total chloride concentration profile under this temperature gradient is shown in Fig. 12. The control mix shows a more regular chloride profile compared to the CNTs-based mixes. Like the compressive strength and absorption test, 0.05% CNTs performed optimally, while the higher CNTs dosages showed a higher concentration profile. Additionally, the total chloride concentration profile becomes more irregular at higher CNTs dosages compared to the optimal mix and the control mix. The enhanced chloride resistance at 0.05% CNTs dosage is attributed to efficient CNTs dosages cause agglomeration, which creates weak zones and favored paths for chloride ingress, resulting in higher and irregular chloride concentration profiles.

Similarly, the chloride concentration profile resembles the absorption rate profile in CNTs-based materials, as chlorides are carried into the cementitious matrix alongside water. Higher CNTs dosages, with higher absorption rates, produce a more erratic chloride concentration profile. This is because, the chloride concentration profile closely follows the absorption rate profile, which becomes progressively erratic with higher CNTs dosages.

Stage II—detailed chloride diffusion analysis of optimal mix

Based on the results of Stage I, the optimal amount was determined to be 0.05% CNTs, which achieved the highest compressive strength while also having the lowest absorption and permeable voids. Furthermore, this mix exhibited improved porosity and the lowest chloride concentration profile under the TG condition. Therefore, the detailed chloride diffusion analysis was conducted for the mix with an optimal dosage of 0.05% CNTs in stage II.

Chloride diffusion under different temperature conditions

Figure 13 shows the total chloride concentration profile along the depth from the chloride exposed surface under different temperature conditions for the optimal mix (0.05% CNTs) in comparison with the control mix.

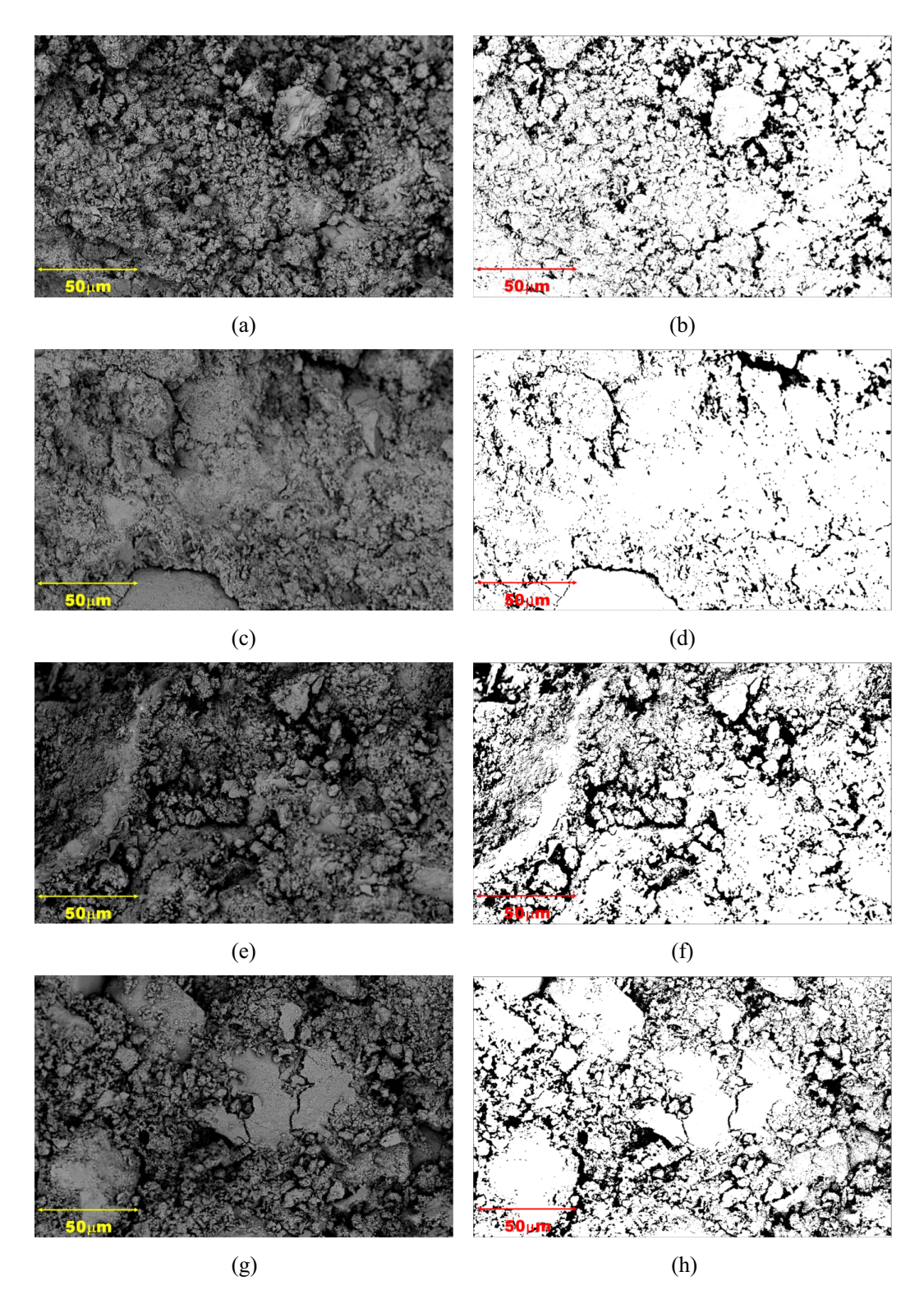


Fig. 10. BSE images (left) and binary BSE images (right) of all the mixes; (a, b) a control mix showing more regular and uniform distribution of pores, (c, d) a mix with 0.05% CNTs showing reduced sizes and non-uniform distribution of pores, (e, f) a mix with 0.10% CNTs showing larger and non-uniformly distributed pores, and (g, h) a mix with 0.15% CNTs showing much larger and non-uniformly distributed pores.

The optimal mix consistently resulted in the lowest chloride content profile under all temperature conditions, including constant room temperature (CT22), constant high temperature of 50 °C (CT50), and TG. It can be seen that chloride concentration increases with the increase in temperature due to the mobility of the chloride ions under the influence of higher temperatures^{7,81,82}. However, the TG condition is the worst case as expected

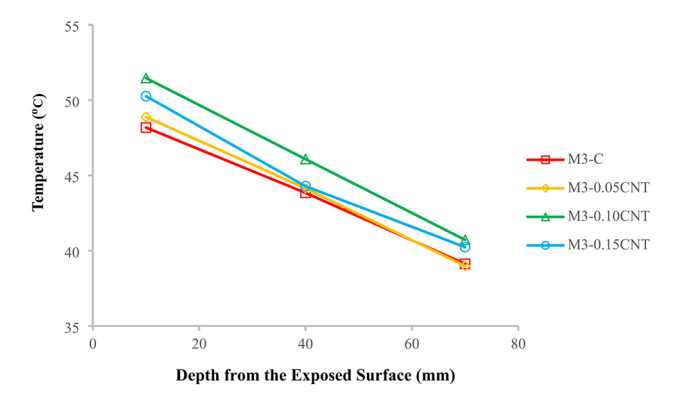


Fig. 11. Variation of temperature through the depth of mortar for all specimens.

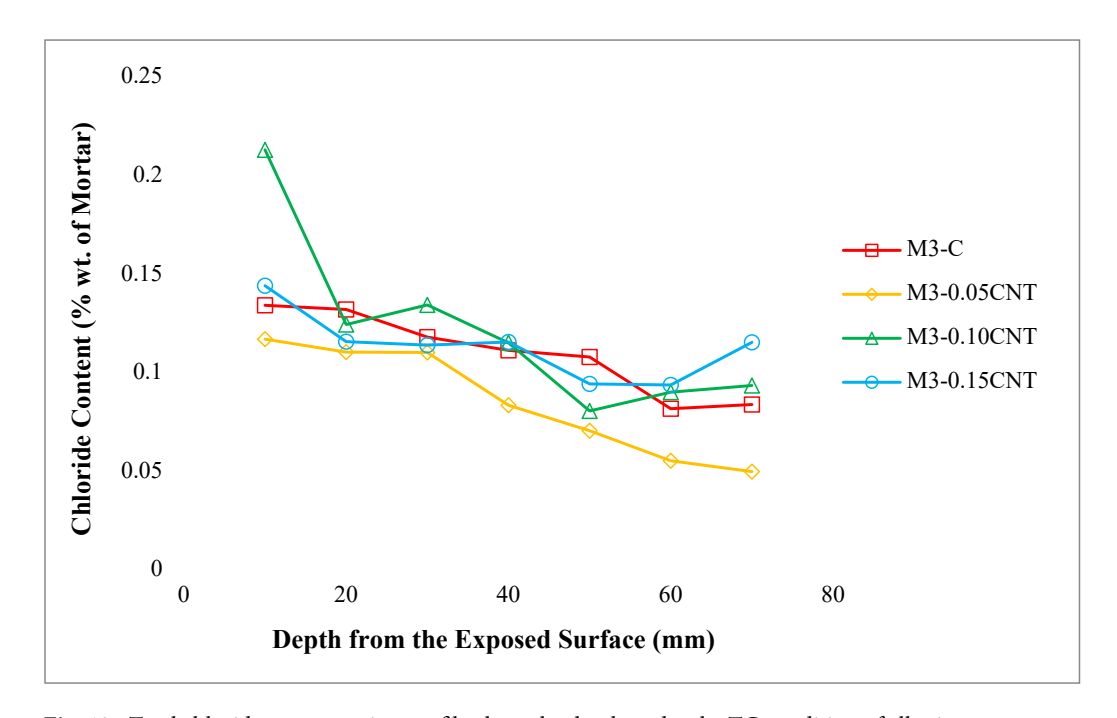
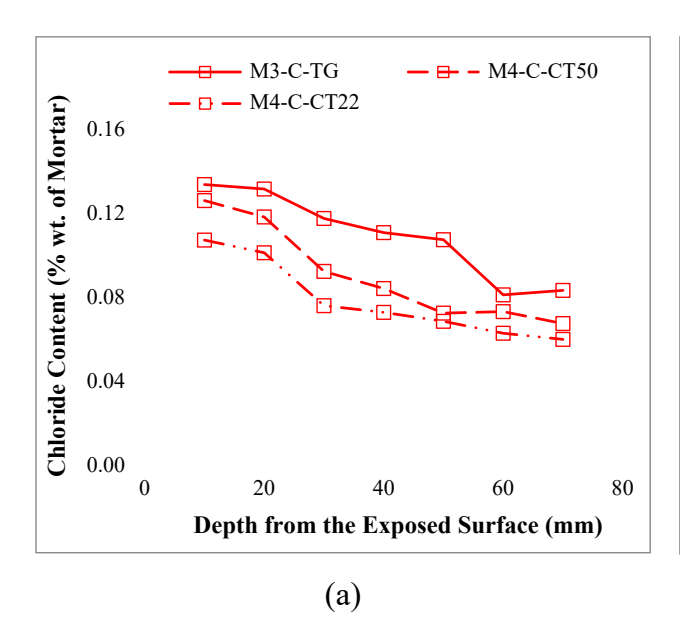


Fig. 12. Total chloride concentration profile along the depth under the TG condition of all mixes.

and shows the highest concentration profile. This is because of the Soret effect in which chloride ions move from a hotter region to a cooler region and cause more concentration of chloride in the cooler region as compared to the constant temperature¹². The differential kinetic energy of chloride ions in both regions compels the chloride ions to move from a hotter region to a cooler region due to a double driving force resulting in both mass diffusion (due to concentration gradient) and thermo-diffusion (due to temperature difference)¹³. Furthermore, Fig. 14 shows the comparative total chloride concentration profile of the optimal mix with the control mix along the depth from the chloride exposed surface for TG, CT50, and CT22 conditions, respectively. These graphs indicate that variation in the chloride contents between the control mix and the optimal mix is relatively small near the chloride exposed surface but becomes significant deeper inside the specimen for all temperature conditions. It indicates slower transportation of chlorides and accordingly less content of chlorides deep inside the specimens due to the presence of CNTs. This reduced chloride penetration is potentially due to the higher tortuosity induced by CNTs, as evident from the absorption results from Fig. 9. Furthermore, this is also evidenced in Fig. 10, which shows a non-uniform distribution of pores in CNTs-based mixes, resulting in increasing tortuosity.

Total chlorides vs. free chlorides

A comparative analysis was conducted on the total chloride content and free chloride concentration profile for both the control mix and the optimal mix under the TG condition, as shown in Fig. 15. The optimal mix releases a higher amount of free chlorides in the pore solution. These free chloride ions may originate from both the cement paste and CNTs. However, the free chloride concentration profile of the optimal mix is steeper than the control mix. These results indicate that there is more concentration of free chlorides in the optimal mix near the chloride exposed surface as compared to the control mix. On the other hand, the condition is completely



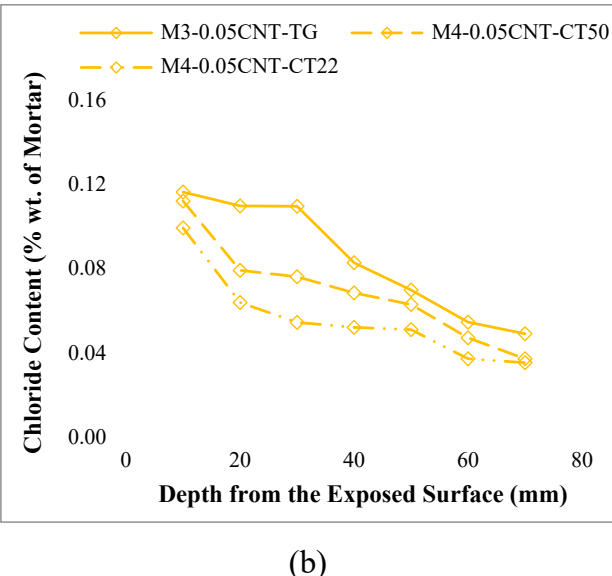
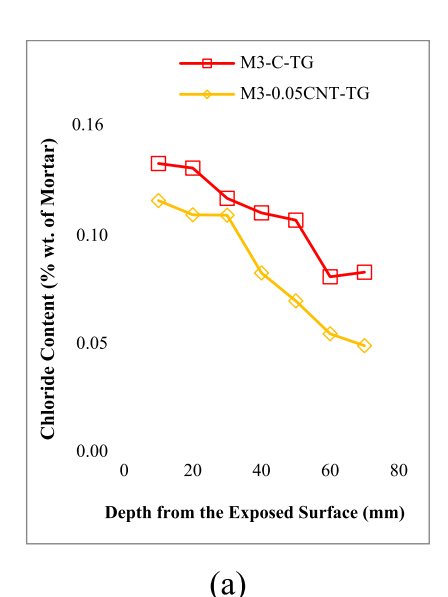
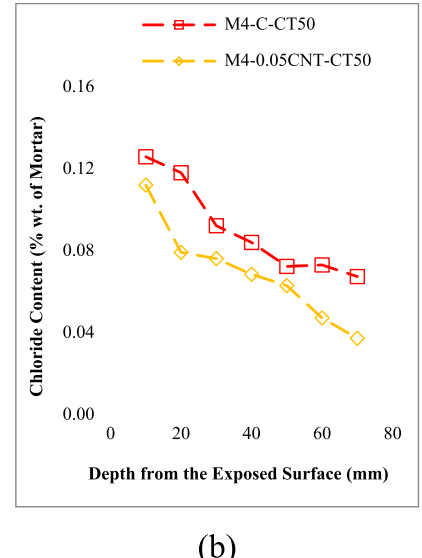


Fig. 13. Total chloride concentration profile along the depth under constant temperature of 22 °C, constant temperature of 50 °C, and TG conditions, (a) control specimen, (b) optimal mixes.





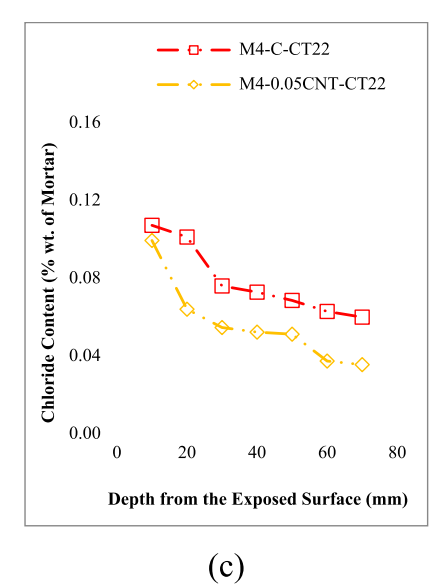


Fig. 14. Comparison of total chloride profile along the depth of the optimal mix with control mix under (a) TG conditions, (b) Constant temperature of 50 °C, and (c) Constant temperature of 22 °C.

opposite to the other (sealed) end of the specimen where the free chloride content is relatively higher in the control mix. Thus, the slope of the free chloride concentration profile is steeper than the control mix. More precisely, there is about more than 50% more free chloride concentration near the chloride exposed surface in the optimal mix than in the control mix, but the control mix shows less than 10% more free chloride content than the optimal mix at the other end as shown below in Fig. 15. Therefore, the higher concentration of free chlorides in the optimal mix near the chloride exposed surface or in the higher temperature zone indicates a higher leaching potential of free chlorides in CNTs based mix.

Based on long-term data, it has been stated in the literature that total chlorides and free chlorides have a linear relationship⁸³. However, the long-term data needed to establish this relationship is not available in the current study. Based on the accelerated experimental results, an attempt has been made to establish a linear relationship between the total chlorides and free chlorides (Fig. 16). The release of free chlorides in the control mix and the mix containing 0.05% CTs under the TG condition can be understood from this moderately strong relationship. There are relatively more free chlorides close to the chloride exposed surface or in the high-temperature zone, as indicated by the steeper slope in the mix containing 0.05% CNTs.

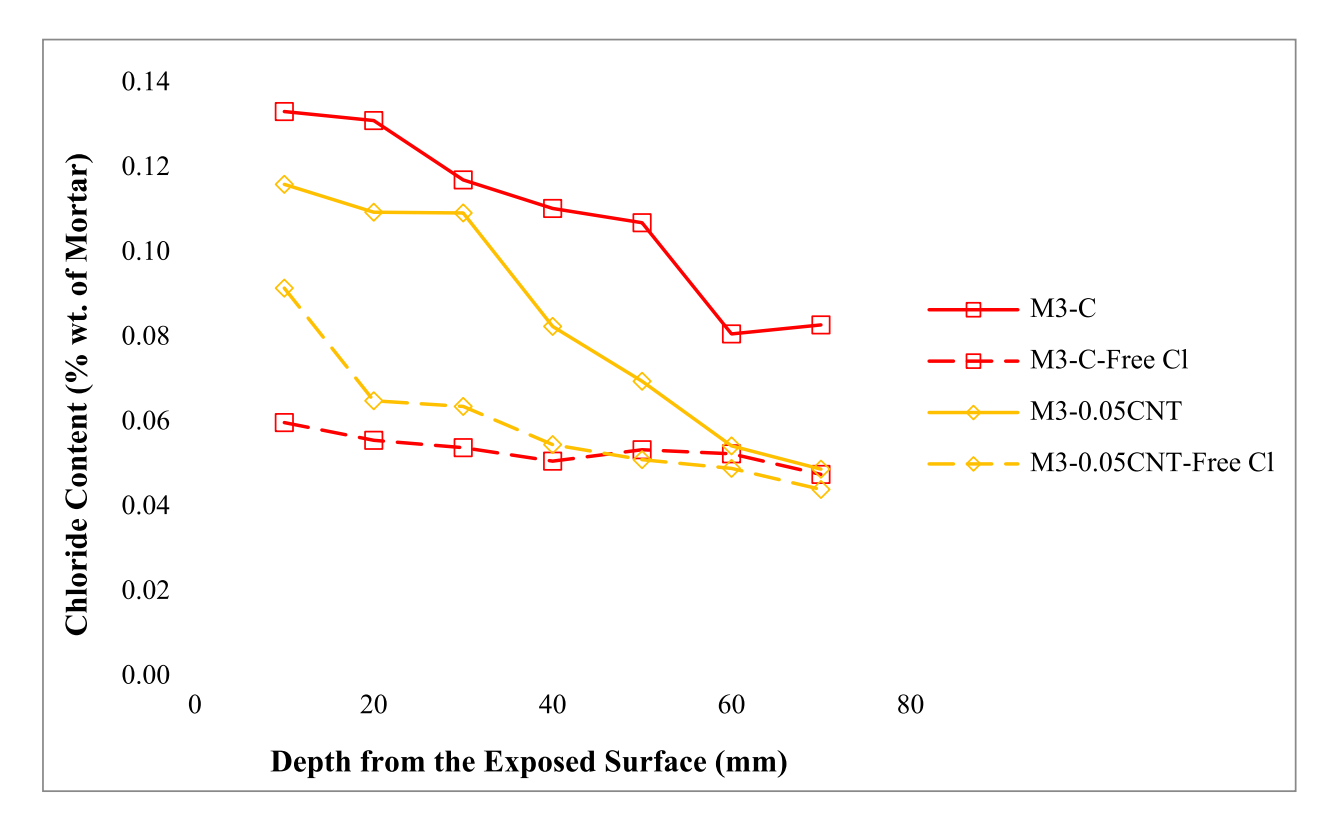


Fig. 15. Total vs. free chloride content under TG condition for both control and optimal mix.

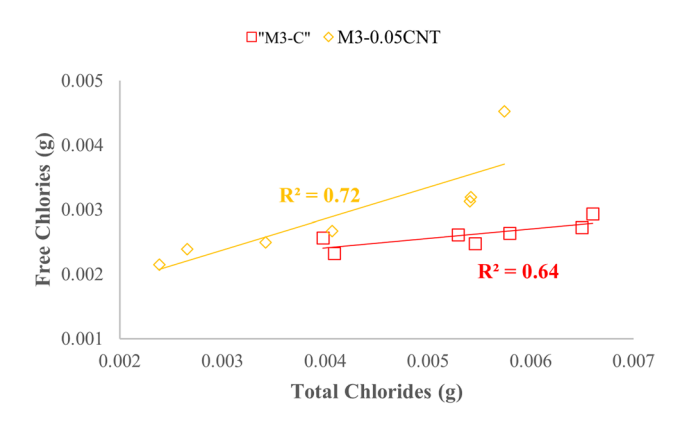
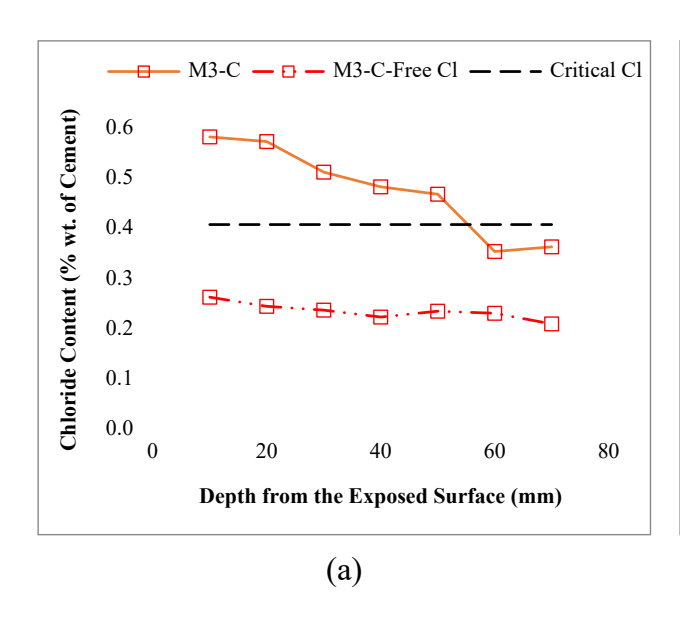


Fig. 16. Linear relationship between free chloride content vs. total chloride content for the control mix and the optimal mix under TG conditions.

Regarding hydrophobicity and hydrophilicity, pristine CNTs are often hydrophobic by nature, hindering their effective dispersion in an aqueous solution. However, they can be rendered hydrophilic by applying surface treatments that are either covalent or non-covalent³⁹. PEG was used in this investigation to treat the CNTs, as shown in Table 3 in Sect. 2. This type of treatment increases the hydrophilicity of CNTs, making them suitable for use in aqueous conditions^{39,40}. As a result, both the absorption properties of the cement paste and the CNTs determine the accessible porosity and overall absorption of water in cement mortar after 72 h, as shown in Fig. 7.

The hydrophilicity of the CNTs used in this study can be relatable to the population of the free chlorides or higher leaching potential of chlorides at the exposed end of the specimen. This higher concentration of free chlorides in this region is justifiable through a study that reports the same phenomenon near the chloride exposed surface in CNTs-based specimens⁸⁴. However, that study did not consider the effect of temperature conditions. Also, PEG when used as a chemical admixture reduces the chloride binding capacity of cement paste by loosening the microstructure⁴¹. Nevertheless, it can be assumed that higher hydrophilicity of CNTs causes the higher absorption of water accompanying the chloride ions. These chloride ions may have been released (leached out) under the influence of elevated temperatures in the high-temperature zone of the specimen under the TG



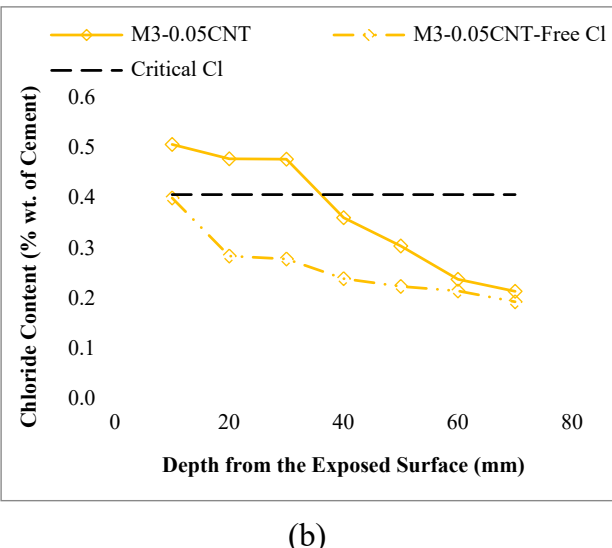


Fig. 17. Comparison of chloride contents of the control and the optimal mix with critical chloride content.

Depth from the exposed surface (mm)	Critical chloride content (% wt of cement)	Control mix (% wt of cement)	Optimal mix (% wt of cement)
10	0.4	0.575	0.500
20	0.4	0.565	0.471
30	0.4	0.504	0.471
40	0.4	0.475	0.354
50	0.4	0.460	0.298
60	0.4	0.346	0.231
70	0.4	0.356	0.207

Table 7. Total chloride content along the depth of the specimen.

condition. To authenticate this hypothesis, a more detailed and precise study is needed that aims at releasing and absorption potential of chlorides by the CNTs in the cementitious mortar.

Corrosion initiation potential

The initiation of corrosion in the reinforcement is determined by the critical chloride content. Once this crucial threshold is achieved, corrosion starts. The threshold chloride content in cementitious materials required to initiate corrosion is a topic of discussion among researchers. Research, for instance, has reported re-examining the critical chloride level while taking non-conventional binders into account³⁷ and the stress conditions of the reinforcement³⁸. Generally, a critical chloride level of 0.4% by weight of cement can be used for investigation³⁶. However, a very aggressive marine environment, such as the Arabian Gulf region, where the seawater salinity and the chloride ions concentration in the atmosphere are very high, has a lower critical chloride content of 0.3%⁸⁵. Some studies indicate that only free chlorides are responsible for corrosion initiation in reinforced concrete^{86,87}. However, a commonly recognized concept proposes that bound chlorides upon interaction with certain factors may become free chlorides and become a part of a pore solution^{88–90}. Although free chlorides are also occasionally taken into consideration, the critical chloride content is often determined by total chloride contents^{69–71}. The profiles of total, free, and bound chlorides, along with the overall critical chloride concentration of 0.4% are shown in Fiure 17, for both the control mix and the optimal mix under the TG condition. Compared to the control mix, the optimal mix exhibits a lower total chloride content, indicating a reduced potential to corrosion initiation.

The experimental results indicate that the critical chloride content had penetrated beyond a depth of 50 mm of the control specimen after 30 days of exposure to a 3% NaCl solution in the laboratory. Additionally, the chloride diffusion resistance of the optimal mix surpasses that of the control mix, attributed to its reduced porosity^{19,71,72} and increased tortuosity⁷⁴. In the optimal mix, the critical chloride content reached depths of less than 40 mm. Detailed total chloride content profiles at various depths for both specimens are presented in Table 7. Furthermore, no depth shows a free chloride content above the critical value in both specimens.

From the outcomes of the current study, the incorporation of CNTs in cementitious materials effectively delays chloride diffusion and, thus, postpones the initiation of corrosion. This enhancement reflects the enhanced durability and extended service life of concrete structures, especially in aggressive environments such as the MENA region, where harsh temperature gradients across concrete sections promote deterioration.

Conclusion

This study explored the impact of CNTs on inhibiting the diffusion of harmful chloride ions in cement mortar, under varying conditions, including low constant room temperature of 22 °C, high ambient temperature of 50 °C, and TG conditions. The key findings of this investigation are summarized as follows:

- A CNTs dosage of 0.05% was identified as the optimal concentration, enhancing both mechanical and durability performance. This dosage increased compressive strength by over 24%, absorption and reduced accessible porosity about 17.50%, refined the pore structure, and significantly lowered the total chloride content across the depth of the specimens under temperature gradient conditions.
- The temperature gradient condition across the section depth proved more detrimental to chloride ion diffusion compared to constant temperature conditions. However, the optimal mix (0.05% CNTs) exhibited lower total chloride content across the depth compared to the control mix under varying conditions, including low constant room temperature of 22 °C, high ambient temperature of 50 °C, and TG conditions. This enhanced resistance is attributed to the reduced porosity and increased tortuosity of the cement mortar due to the addition of CNTs.
- The optimal mix (0.05% CNTs) released more free chloride ions compared to the control mix, attributed to the high hydrophilicity of the PEG-treated CNTs used in this study. These CNTs absorb chloride ions along with water and gradually release them as free chloride ions under high temperatures. This phenomenon can be observed near the exposed surface and less noticeable in deeper regions of the cement mortar. Despite this localized effect, the total chloride content in the CNTs-mix remained lower than in the control mix, although the gradient of free chloride content was steeper along the depth.
- The optimal mix (0.05% CNTs) can effectively delay chloride ion diffusion and consequently the initiation of
 corrosion due to increased tortuosity and reduced porosity. This mix provides resistance to critical chloride
 ingress, even under temperature gradient conditions, indicating its robustness and integrity in the aggressive
 environment where temperature gradients are common during peak summers.

Based on the findings, this study can be extended for further investigation. It is recommended to compare the performance of pristine and functionalized/treated CNTs for chloride diffusion, including both total and free chlorides, under different temperature conditions. The effect of the w/b ratio, along with different dosages of CNTs, can also be considered in this regard. Ultimately, a comparative study is also recommended to evaluate the chloride diffusion resistance potential of cementitious composites incorporating CNTs and other carbon-based nanomaterials, such as graphene, to determine the most effective nanomaterial.

Data availability

The datasets used and/or analysed during the current study available from the corresponding author on reasonable request.

Received: 25 March 2025; Accepted: 23 May 2025

Published online: 01 June 2025

References

- 1. Basheer, P., Chidiac, S. E. & Long, A. E. Predictive models for deterioration of concrete structures. *Constr. Build. Mater.* 10, 27–37 (1996).
- 2. Ahmad, X. A. & Kumar, A. Chloride ion migration/diffusion through concrete and test methods. *Int. J. Adv. Sci. Tech. Res.* 6, 151–180 (2013).
- 3. Hodhod, O. A. & Ahmed, H. I. Modeling the service life of slag concrete exposed to chlorides. *Ain Shams Eng. J.* 5, 49–54. https://doi.org/10.1016/j.asej.2013.08.001 (2014).
- 4. Stanish, K. D. *Testing the Chloride Penetration Resistance of Concrete: A Literature Review* (University of Toronto, Department of Civil Engineering; Federal Highway Administration, Turner-Fairbank Highway Research Center, 1997).
- 5. Roa-Rodriguez, G., Aperador, W. & Delgado, A. Calculation of chloride penetration profile in concrete structures. *Int. J. Electrochem. Sci.* 8, 5022–5035 (2013).
- Angst, U., Elsener, B., Larsen, C. K. & Vennesland, Ø. Critical chloride content in reinforced concrete—A review. Cem. Concr Res. 39, 1122–1138. https://doi.org/10.1016/j.cemconres.2009.08.006 (2009).
- 7. Yuan, Q., Shi, C., De Schutter, G. & Audenaert, K. Effect of temperature on transport of chloride ions in concrete. In *Concrete Repair, Rehabilitation and Retrofitting II* 177–178 (2008).
- 8. Dousti, X. A. & Shekarchi, M. Effect of exposure temperature on chloride-binding capacity of cementing materials. *Mag. Concr. Res.* 67, 821–832. https://doi.org/10.1680/macr.14.00327 (2015).
- 9. An, X. B. et al. Effect of temperature gradient on chloride ion diffusion in nuclear reactor containment Building concrete. *Energies* (*Basel*). 15, 1–14. https://doi.org/10.3390/en15155581 (2022).
- Shittu, R. et al. Chloride diffusion in concrete under temperature gradient condition in arid climates. In Proceedings of the 8th International Conference on Civil Structural and Transportation Engineering (ICCSTE'23), Canada. https://doi.org/10.11159/iccste 23.165 (2023).
- 11. Shittu, R. et al. Influence of mix design on chloride diffusion in concrete structures under temperature gradient conditions. In 9th World Congress on Civil, Structural, and Environmental Engineering, CSEE 2024 (2024).
- 12. Soret, C. Sur l'état d'équilibre Que prend Au point de vue de Sa concentration Une dissolution Saline primitivement homogène dont Deux parties Sont Portées a des températures difféntes. *Arch. Sci. Phys. Nat.* 2, 48 (1879).
- 13. Platten, J. K. The Soret effect: A review of recent experimental results. J. Appl. Mech. Trans. ASME. 73, 5–15. https://doi.org/10.11 15/1.1992517 (2006).
- 14. Han, B., Yang, Z., Shi, X. & Yu, X. Transport properties of carbon-nanotube/cement composites. J. Mater. Eng. Perform. 22, 184–189. https://doi.org/10.1007/s11665-012-0228-x (2013).
- Alafogianni, P., Dassios, K., Tsakiroglou, C. D., Matikas, T. E. & Barkoula, N. M. Effect of CNT addition and dispersive agents on the transport properties and microstructure of cement mortars. Constr. Build. Mater. 197, 251–261. https://doi.org/10.1016/j.conb uildmat.2018.11.169 (2019).

- 16. Ali, M. M. et al. Influence of carbon nanotubes on printing quality and mechanical properties of 3D printed cementitious materials. Developments Built Environ. 18, 100415. https://doi.org/10.1016/j.dibe.2024.100415 (2024).
- 17. Ali, M. M., Abu Al-Rub, R. K., Banat, F. & Kim, T. Y. Enhancing the printing quality and mechanical properties of 3D-printed cement composites with date syrup-based graphene coated sand hybrid. *Developments Built Environ.* 20, 100582. https://doi.org/10.1016/j.dibe.2024.100582 (2024).
- 18. Li, G. Y., Wang, P. M. & Zhao, X. Mechanical behavior and microstructure of cement composites incorporating surface-treated multi-walled carbon nanotubes. *Carbon N Y.* 43, 1239–1245. https://doi.org/10.1016/j.carbon.2004.12.017 (2005).
- Carriço, X. A., Bogas, J. A., Hawreen, A. & Guedes, M. Durability of multi-walled carbon nanotube reinforced concrete. Constr. Build. Mater. 164, 121–133. https://doi.org/10.1016/j.conbuildmat.2017.12.221 (2018).
- Meddah, M. S., Praveenkumar, T. R., Vijayalakshmi, M. M., Manigandan, S. & Arunachalam, R. Mechanical and microstructural characterization of rice husk Ash and Al2O3 nanoparticles modified cement concrete. *Constr. Build. Mater.* 255, 119358. https://doi.org/10.1016/j.conbuildmat.2020.119358 (2020).
- Zhang, M. & Li, H. Pore structure and chloride permeability of concrete containing nano-particles for pavement. Constr. Build. Mater. 25, 608–616. https://doi.org/10.1016/j.conbuildmat.2010.07.032 (2011).
- Wang, B. & Zhao, R. Effect of graphene nano-sheets on the chloride penetration and microstructure of the cement based composite. Constr. Build. Mater. 161, 715–722. https://doi.org/10.1016/j.conbuildmat.2017.12.094 (2018).
- 23. Galao, O., Zornoza, E., Baeza, F. J., Bernabeu, A. & Garcés, P. Effect of carbon nanofiber addition in the mechanical properties and durability of cementitious materials. *Materiales De Construccion.* **62**, 343–357. https://doi.org/10.3989/mc.2012.01211 (2012).
- 24. Lee, J., Mahendra, S. & Alvarez, P. J. J. Nanomaterials in the construction industry: a review of their applications and environmental health and safety considerations. ACS Nano. 4, 3580–3590 (2010).
- 25. Holman, M. Nanomaterial Forecast: Vols and Applications, ICON Nanomaterial Environmental Health and Safety Research Needs
 Assessment (Lux Research, 2007).
- 26. Rashad, A. M. Effect of carbon nanotubes (CNTs) on the properties of traditional cementitious materials. *Constr. Build. Mater.* 153, 81–101. https://doi.org/10.1016/j.conbuildmat.2017.07.089 (2017).
- Dalla, P. T. et al. Effect of carbon nanotubes on chloride penetration in cement mortars. Appl. Sci. (Switzerland). 9, 19–22. https://doi.org/10.3390/app9051032 (2019).
- 28. Panagiotakopoulou, C., Papandreopoulos, P. & Batis, G. Investigation of corrosion protection through CNTs/ CNFs modified cement mortars. *Curr. Nanomaterials.* 9, 266–278. https://doi.org/10.2174/2405461508666230901123920 (2024).
- Chukka, N. D. K. R. et al. Experimental testing on mechanical, durability, and adsorption dispersion properties of concrete with multiwalled carbon nanotubes and silica fumes. Adsorpt. Sci. Technol. 1, 1–13. https://doi.org/10.1155/2022/4347753 (2022).
- 30. Lu, L., Ouyang, D. & Xu, W. Mechanical properties and durability of ultra high strength concrete incorporating multi-walled carbon nanotubes. *Materials* **9**, 1–11. https://doi.org/10.3390/ma9060419 (2016).
- Rafieizonooz, M. Effect of Carbon Nanotubes on Chloride Diffusion, Strength, and Microstructure of Ultra-High Performance Lightweight Concrete. https://doi.org/10.2139/ssrn.4772358 (2024).
- 32. Yu, F., Sun, T., Dong, S., Ding, S. & Han, B. Chloride penetration resistance of ultra-high performance concrete with various multiwalled carbon nanotubes. *Constr. Build. Mater.* **421**, 135751. https://doi.org/10.1016/j.conbuildmat.2024.135751 (2024).
- 33. Mohsen, M. O., Al-Nuaimi, N., Abu Al-Rub, R. K., Senouci, A. & Bani-Hani, K. A. Effect of mixing duration on flexural strength of multi walled carbon nanotubes cementitious composites. *Constr. Build. Mater.* 126, 586–598. https://doi.org/10.1016/j.conbuild mat.2016.09.073 (2016).
- 34. Hu, J. Porosity of Concrete—Morphological Study of Model Concrete, TU Delft. https://www.narcis.nl/publication/RecordID/oai:tu delft.nl:uuid:7ec84b76-d120-48f7-96a4-b68de2463154 (2004).
- Scrivener, K. L. & Nonat, A. Hydration of cementitious materials, present and future. Cem. Concr Res. 41, 651–665. https://doi.org/10.1016/j.cemconres.2011.03.026 (2011).
- 36. Le Bellégo, C., Pijaudier-Cabot, G., Gérard, B., Dubé, J. F. & Molez, L. Coupled mechanical and chemical damage in calcium leached cementitious structures. J. Eng. Mech. 129, 333–341. https://doi.org/10.1061/(asce)0733-9399(2003)129:3(333) (2003).
- Sáez, Y., De Ibarra, J. J., Gaitero, E., Erkizia, I. & Campillo Atomic force microscopy and nanoindentation of cement pastes with nanotube dispersions. *Phys. Status Solidi (A) Appl. Mater. Sci.* 203, 1076–1081. https://doi.org/10.1002/pssa.200566166 (2006).
- 38. Collins, F., Lambert, J. & Duan, W. H. The influences of admixtures on the dispersion, workability, and strength of carbon nanotube-OPC paste mixtures. Cem. Concr Compos. 34, 201-207. https://doi.org/10.1016/j.cemconcomp.2011.09.013 (2012).
- 39. Gao, C. et al. Surface modification methods and mechanisms in carbon nanotubes dispersion. Carbon NY. 212, 118133. https://doi.org/10.1016/j.carbon.2023.118133 (2023).
- Manasrah, A. D., Laoui, T., Zaidi, S. J. & Atieh, M. A. Effect of PEG functionalized carbon nanotubes on the enhancement of thermal and physical properties of nanofluids. *Exp. Therm. Fluid Sci.* 84, 231–241. https://doi.org/10.1016/j.expthermflusci.2017.0 2.018 (2017).
- 41. Zhao, L., Feng, P., Ye, S., Liu, X. & Wang, H. Effect of polyethylene glycol on chloride binding in mortar. Constr. Build. Mater. 311, 125321. https://doi.org/10.1016/j.conbuildmat.2021.125321 (2021).
- 42. Güler, Ö., Cacim, N. N., Evin, E. & Yahia, I. S. The synergistic effect of CNTs-polymeric surfactant on the properties of concrete nanocomposites: comparative study. *J. Compos. Mater.* 55, 1371–1384. https://doi.org/10.1177/0021998320971346 (2021).
- 43. Daoust, K., Vallières, P. L., Tagnit-Hamou, A. & Claverie, J. P. Carbon nanofibers encapsulated by polyethylene glycol increase the mechanical properties and durability of OPC mortars. *Constr. Build. Mater.* 447. https://doi.org/10.1016/j.conbuildmat.2024.137986 (2024).
- 44. World Data. Climate in Emirates. https://www.worlddata.info/asia/arab-emirates/climate-abu-dhabi.php (Accessed 26 April 2023)
- Nassrullah, G. et al. Optimizing cement-based material formulation for 3D printing: integrating carbon nanotubes and silica fume. Case Stud. Constr. Mater. 22, e04579. https://doi.org/10.1016/j.cscm.2025.e04579 (2025).
- 46. ASTM. Standard Test Method for Sieve Analysis of Fine and Coarse Aggregates—ASTM C136/C136M-19. https://doi.org/10.1520/C0136 (2019).
- 47. Abu Seif, E. S. S., Sonbul, A. R., Hakami, B. A. H. & El-Sawy, E. K. Experimental study on the utilization of Dune sands as a construction material in the area between Jeddah and Mecca, Western Saudi Arabia. *Bull. Eng. Geol. Environ.* 75, 1007–1022. https://doi.org/10.1007/s10064-016-0855-9 (2016).
- 48. Maza, M., Naceri, A. & Zitouni, S. Physio-mechanical properties of mortar made with binary natural fine aggregates (dune sand and crushed sand) with and without admixtures. *Asian J. Civil Eng.* 17, 663–682 (2016).
- Lee, E., Park, S. & Kim, Y. Drying shrinkage cracking of concrete using Dune sand and crushed sand. Constr. Build. Mater. 126, 517–526. https://doi.org/10.1016/j.conbuildmat.2016.08.141 (2016).
- 50. ASTM. Standard Specification for Chemical Admixtures for Concrete—C494/C494M, Annual Book of ASTM Standards 04 1-9 1-9. https://doi.org/10.1520/C0494 (2019).
- 51. ASTM. Standard Test Method for Acid Soluble Chloride in Mortar and Concrete—C1152/C1152M (ASTM International, 2020).
- 52. ASTM. Standard Test Method for Water-Soluble Chloride in Mortar and Concrete—C1218/C1218M 1 (ASTM International, 2020).
- ASTM. Standard Test Method for Compressive Strength of Hydraulic Cement Mortars—C109/C109M, Annual Book of ASTM Standards (23AD). https://doi.org/10.1520/C0109
- 54. ASTM. Standard Test Method for Flow of Hydraulic Cement Mortar—C1437, Annual Book of ASTM Standards. https://doi.org/10.1520/C1437-20.2 (2020).

- Kan, D., Liu, G., Cao, S. C., Chen, Z. & Lyu, Q. Mechanical properties and pore structure of multiwalled carbon nanotubereinforced reactive powder concrete for three-dimensional printing manufactured by material extrusion. 3D Print. Addit. Manuf. 11, e675–e687. https://doi.org/10.1089/3dp.2022.0243 (2022).
- Sun, T. et al. High-durability, low carbon, and low-cost nano-engineered concrete for marine concrete infrastructures. Cem. Concr. Compos. 157, 105877. https://doi.org/10.1016/j.cemconcomp.2024.105877 (2025).
- 57. An, B. et al. Effect of temperature gradient on chloride ion diffusion in nuclear reactor containment Building concrete. *Energies (Basel)*. 15, 1–14. https://doi.org/10.3390/en15155581 (2022).
- 58. Shittu, R. A. Influence of High Ambient Temperature on Chloride Penetration into Nuclear Reactor Containment Buildings Influence of High Ambient Temperature on Chloride Penetration into Nuclear Reactor Containment Buildings (Khalifa University, 2023).
- 59. Maqsood, S. Effect of Carbon Nanotubes on Chloride Diffusion in Cementitious Materials Under the Marine Environment of the Arabian Gulf. https://doi.org/10.13140/RG.2.2.35801.84322 (Khalifa University, 2024).
- 60. Wang, Y. et al. Factors influencing the capillary water absorption characteristics of concrete and their relationship to pore structure. *Appl. Sci. (Switzerland)*. 12, 2211. https://doi.org/10.3390/app12042211 (2022).
- 61. Angelin, A. F., Lintz, R. C. C., Gachet-Barbosa, L. A. & Osório, W. R. The effects of porosity on mechanical behavior and water absorption of an environmentally friendly cement mortar with recycled rubber. *Constr. Build. Mater.* 151, 534–545. https://doi.org/10.1016/j.conbuildmat.2017.06.061 (2017).
- 62. Huynh, T. P., Vo, D. H. & Hwang, C. L. Engineering and durability properties of eco-friendly mortar using cement-free SRF binder. Constr. Build. Mater. 160, 145–155. https://doi.org/10.1016/j.conbuildmat.2017.11.040 (2018).
- 63. ABNT. ABNT NBR 9778: Hardened Mortar and Concrete—Determination of Water Absorption, Voids Index, and Specific Mass (Associação Brasileira de Normas Técnicas, 2009).
- 64. Li, Z. Materials for making concrete. In Advanced Concrete Technology 23-92 (Wiley, 2011).
- 65. Tao, S. & Yumei, Y. Quantitative analysis of ettringite formed in the hydration products of high-alite cements. *Adv. Cem. Res.* 27, 497–505. https://doi.org/10.1680/adcr.14.00054 (2015).
- 66. Taylor, H. F. W. Hydration of Portland cement. In Cement Chemistry, 2nd edn., 187-225 (Thomas Telford, 1997).
- 67. Luccioni, B. M., Figueroa, M. I. & Danesi, R. F. Thermo-mechanic model for concrete exposed to elevated temperatures. *Eng. Struct.* 25, 729–742. https://doi.org/10.1016/S0141-0296(02)00209-2 (2003).
- 68. Flint, L. E. & Flint, A. L. 2.3 Porosity, Methods of Soil Analysis: Part 4 Physical Methods, vol. 5, 241–254 (2002).
- Khitab, X. A. et al. Fracture toughness and failure mechanism of high performance concrete incorporating carbon nanotubes. Frattura Ed. Integrita Strutturale. 11, 238–248. https://doi.org/10.3221/IGF-ESIS.42.26 (2017).
- 70. Gillani, S. S. U. H. et al. Improving the mechanical performance of cement composites by carbon nanotubes addition. *Procedia Struct. Integr.* **3**, 11–17. https://doi.org/10.1016/j.prostr.2017.04.003 (2017).
- Konsta-Gdoutos, M. S., Metaxa, Z. S. & Shah, S. P. Multi-scale mechanical and fracture characteristics and early-age strain capacity
 of high performance carbon nanotube/cement nanocomposites. Cem. Concr Compos. 32, 110–115. https://doi.org/10.1016/j.cemc
 oncomp.2009.10.007 (2010).
- 72. Hu, Y., Luo, D., Li, P., Li, Q. & Sun, G. Fracture toughness enhancement of cement paste with multi-walled carbon nanotubes. *Constr. Build. Mater.* 70, 332–338. https://doi.org/10.1016/j.conbuildmat.2014.07.077 (2014).
- 73. Nochaiya, T. & Chaipanich, A. Behavior of multi-walled carbon nanotubes on the porosity and microstructure of cement-based materials. *Appl. Surf. Sci.* 257, 1941–1945. https://doi.org/10.1016/j.apsusc.2010.09.030 (2011).
- MacLeod, A. J. N., Gates, W. P. & Collins, F. Durability characterisation of Portland cement-carbon nanotube nanocomposites. *Materials* 13, 1–21. https://doi.org/10.3390/ma13184097 (2020).
- 75. Odler, X. I. & Robler, M. Investigations on the relationship between porosity structure and strength of hydrated Portland cement pastes II. Effect of pore structure and of degree of hydration. *Cem. Concr Res.* 15, 401–410. https://doi.org/10.1016/0008-8846(87) 90054-8 (1985).
- 76. Kearsley, E. P. & Wainwright, P. J. The effect of porosity on the strength of foamed concrete. Cem. Concr. Res. 32, 233–239 (2002).
- Łaźniewska-piekarczyk, B. Investigatons on the relationship between porosity and strength of admixtures modified high performance self-compacting concrete. J. Civil Eng. Manage. 22, 520–528. https://doi.org/10.3846/13923730.2014.897978 (2016).
- Yaman, I. O., Hearn, N. & Aktan, H. M. Active and non-active porosity in concrete. Experimental Evid. Mater. Struct. 35, 102–109. https://doi.org/10.1007/bf02482110 (2002).
- 79. Luan, Y. & Tetsuya, I. A multi-scale approach for simulation of capillary absorption of cracked SHCC based on crack pattern and water status in micropores. *Mater. Struct.* 54, 1–15. https://doi.org/10.1617/s11527-021-01664-3 (2021).
- 80. Holzer, L. et al. Review of theories and a new classification of tortuosity types. In *Tortuosity and Microstructure Effects in Porous Media*, 1st edn., 7–50. https://doi.org/10.1007/978-3-031-30477-4 (Springer, 2023).
- 81. Touil, B., Ghomari, F., Bezzar, A., Khelidj, A. & Bonnet, S. Effect of temperature on chloride diffusion in saturated concrete. *ACI Mater. J.* 114, 713–721. https://doi.org/10.14359/51688929 (2017).
- 82. Hu, S., Peng, J., Zhang, J. & Cai, C. S. Influences of time, temperature, and humidity on chloride diffusivity: mesoscopic numerical research. *J. Mater. Civ. Eng.* 29, 80. https://doi.org/10.1061/(asce)mt.1943-5533.0002080 (2017).
- 83. Mohammed, T. U. & Hamada, H. Relationship between free chloride and total chloride contents in concrete. Cem. Concr Res. 33, 1487–1490. https://doi.org/10.1016/S0008-8846(03)00065-6 (2003).
- 84. Han, Y. et al. Chloride ion penetration resistance of matrix and interfacial transition zone of multi-walled carbon nanotube-reinforced concrete. J. Building Eng. 72, 106587. https://doi.org/10.1016/j.jobe.2023.106587 (2023).
- 85. Matta, Z. G. Chlorides and corrosion in the Arabian Gulf environment. Concr. Int. 14, 1 (1992).
- 86. Suryavanshi, A. K., Scantlebury, J. D. & Lyon, S. B. Corrosion of reinforcement steel embedded in high water-cement ratio concrete contaminated with chloride. Cem. Concr Compos. 20, 263–281. https://doi.org/10.1016/S0958-9465(98)00018-3 (1998).
- 87. Kayyali, O. A. & Haque, M. N. The C1-/OH-ratio in chloride-contaminated concrete—a most important criterion. *Magazine Concrete Res.* 47, 235–242. https://doi.org/10.1680/macr.1995.47.172.235 (1995).
- 88. Reddy, B., Glass, G. K., Lim, P. J. & Buenfeld, N. R. On the corrosion risk presented by chloride bound in concrete. *Cem. Concr Compos.* 24, 1–5. https://doi.org/10.1016/S0958-9465(01)00021-X (2002).
- 89. Glass, G. K. & Buenfeld, N. R. The influence of chloride binding on the chloride induced corrosion risk in reinforced concrete. *Corros. Sci.* 42, 329–344. https://doi.org/10.1016/S0010-938X(99)00083-9 (2000).
- Glass, G. K. & Buenfeld, N. R. The presentation of the chloride threshold level for corrosion of steel in concrete. Corros. Sci. 39, 1001–1013. https://doi.org/10.1016/S0010-938X(97)00009-7 (1997).

Acknowledgements

The authors acknowledge the financial support provided by Khalifa University of Science & Technology and Advanced Digital & Additive Manufacturing (ADAM) Group (No. 8474000163).

Author contributions

Conceptualization, T.K.; Methodology, S.M. and T.K.; Experimental work, S.M. and R.S.; Validation, S.M.; Investigation, S.M.; Resources, T.K.; Writing—original draft preparation, S.M.; Writing—review and editing, M.A., R.S., T.K.; Visualization, S.M. and M.A.; Supervision, T.K.; Project administration, T.K; Funding acquisition,

T.K. All authors have read and agreed to the published version of the manuscript.

Declarations

Competing interests

The authors declare no competing interests.

Additional information

Correspondence and requests for materials should be addressed to T.-Y.K.

Reprints and permissions information is available at www.nature.com/reprints.

Publisher's note Springer Nature remains neutral with regard to jurisdictional claims in published maps and institutional affiliations.

Open Access This article is licensed under a Creative Commons Attribution-NonCommercial-NoDerivatives 4.0 International License, which permits any non-commercial use, sharing, distribution and reproduction in any medium or format, as long as you give appropriate credit to the original author(s) and the source, provide a link to the Creative Commons licence, and indicate if you modified the licensed material. You do not have permission under this licence to share adapted material derived from this article or parts of it. The images or other third party material in this article are included in the article's Creative Commons licence, unless indicated otherwise in a credit line to the material. If material is not included in the article's Creative Commons licence and your intended use is not permitted by statutory regulation or exceeds the permitted use, you will need to obtain permission directly from the copyright holder. To view a copy of this licence, visit https://creativecommons.org/licenses/by-nc-nd/4.0/.

© The Author(s) 2025